

The derived alignment between the dipole and rotational axes constitutes a perplexing observation. On Jupiter there exists a strong longitudinal control of the probability of detecting decametric radio bursts; it is reasonable to expect, however, that this will not be the case for Saturn. Thus the lack of longitudinally varying features in the radio spectrum would parallel the observed lack of significant longitudinal features in the planet's atmosphere, as seen in the visible spectrum. Determining Saturn's rotation period with an accuracy comparable to that of Jupiter may be extremely difficult.

The axisymmetrical and dipolar field suggests that, in the inner magnetosphere, charged particle sweeping effects by satellites and particulate rings should have sharp and spatially limited boundaries when observed from a spacecraft in a flyby trajectory, as well as being extremely stable because longitudinally varying radial disturbances are absent. In addition, in an axisymmetrical dipolar field, the radial extent of the L shell regions associated with satellites or particulate rings, where particle absorption effects are observed, is determined by the physical dimensions of the satellite or ring as well as by its orbital eccentricity since the magnetic dipole axis coincides with the focal point of the orbit. This interpretation of course assumes that radial diffusion processes have a characteristic time scale that is long compared with the bounce and drift periods of energetic particles in the L shells.

Thus, a centered dipole field at the planet, aligned with the rotation axis, results in the minimum possible radial extent for the absorption regions. A more complex field, or the representation of the field as an offset tilted dipole, would result in wider absorption regions (unless of course the offset is along the dipole axis) since the range of L shells swept by the satellite or ring as the planet rotates would be increased. Thus, the observed radial extent and symmetry of sweeping effects of satellite and particulate ring impose a maximum bound on the equatorial offset, which can be physically justified in an offset, tilted dipole representation of the planetary magnetic field.

For the planetary dynamo theory, the near alignment between the magnetic and rotation axes further illustrates the apparent paradox associated with Cowling's theorem and the generation of planetary fields by the dynamo mechanism. This theorem states that an axisymmetric flow cannot generate a self-regenerative dynamo, but Braginsky (12)

has shown that small deviations from axisymmetry can lead to dynamo-generated fields if the magnetic Reynolds number is sufficiently high. Thus, the observed near alignment at Saturn may provide an important new constraint for models of planetary dynamos. This constraint was previously unsuspected because, in all magnetic planets for which in situ observations were available before the Saturn encounter, the angle observed between the magnetic and rotational axes has typically been of the order of 10° (13).

The Saturn satellite Titan is among one of the most interesting "lunar" objects in the solar system because of its large size and measurable atmosphere. Conventional estimates of the strength of the planetary field combined with estimates of the solar wind momentum flux at 10 AU had indicated that Titan was always immersed deeply within the Saturnian magnetosphere, because the average distance to the magnetopause was estimated to be $40 R_s$. The Pioneer 11 results, however, estimate the average position to the magnetopause to be approximately $20 R_s$, equal to the orbital radius of Titan. Hence, Titan will be located within the outer magnetosphere, the magnetosheath of Saturn, or even the interplanetary medium. Titan is thus subjected for an appreciable fraction of time to the depositional-erosional effects of a subsonic or supersonic but highly thermalized solar wind. Titan's environment is expected to be much more variable than was previously anticipated.

The Voyager 1 spacecraft will pass within 7000 km of Titan on 11 November 1980 at a local (Saturn) time of approximately 1400 hours. Because of the possible fluctuating character of the environment, deductions of Titan's physical properties may be much more difficult for the fields and particles experiments measuring in situ.

MARIO H. ACUÑA

NORMAN F. NESS

Laboratory for Extraterrestrial Physics,
NASA/Goddard Space Flight Center,
Greenbelt, Maryland 20771

References and Notes

1. M. H. Acuña and N. F. Ness, *Space Sci. Instrum.* **1**, 177 (1975).
2. E. J. Smith, *Jet Propulsion Laboratory Tech. Rep.* 616-48 (1973).
3. F. Sturms, *Jet Propulsion Laboratory Rep.* 32-1503 (1971).
4. M. H. Acuña and N. F. Ness, in *Magnetospheric Particles and Fields*, B. M. McCormac, Ed. (Reidel, Dordrecht, Netherlands, 1976), pp. 311-325.
5. W. Fillius, W. H. Ip, C. E. McIlwain, *Science* **207**, 425 (1980).
6. J. H. Trainor, F. B. McDonald, A. W. Schardt, *ibid.*, p. 421.
7. J. A. Simpson, T. S. Bastian, D. L. Chenette, G. A. Lentz, R. B. McKibben, K. R. Pyle, A. J. Tuzzolino, *ibid.*, p. 411.
8. J. A. Van Allen, M. F. Thomsen, B. A. Randall, R. L. Rairden, C. L. Grosskreutz, *ibid.*, p. 415.
9. F. H. Busse, in *Solar System Plasma Physics*, C. F. Kennel, L. J. Lanzerotti, E. N. Parker, Eds. (North-Holland, Amsterdam, 1979).
10. M. L. Kaiser and R. G. Stone, *Science* **189**, 285 (1975).
11. W. B. Hubbard and R. Smoluchowski, *Space Sci. Rev.* **14**, 599 (1973).
12. S. I. Braginsky, *Geomag. Aeron.* **15**, 127 (1975).
13. N. F. Ness, *Moon Planets* **18**, 427 (1978).
14. We thank D. Stillwell and J. Lepetch for their efforts in implementing the experiment. We also thank R. Thompson, F. W. Ottens, G. Burgess and J. Connerney for their prompt analysis of these data.

3 December 1979

Vertical Structure of the Ionosphere and Upper Neutral Atmosphere of Saturn from the Pioneer Radio Occultation

Abstract. *Radio occultation measurements at S band (2.293 gigahertz) of the ionosphere and upper neutral atmosphere of Saturn were obtained during the flyby of the Pioneer 11 Saturn spacecraft on 5 September 1979. Preliminary analysis of the occultation exit data taken at a latitude of $9.5^\circ S$ and a solar zenith angle of 90.6° revealed the presence of a rather thin ionosphere, having a main peak electron density of about 9.4×10^3 per cubic centimeter at an altitude of about 2800 above the level of a neutral number density of 10^{19} per cubic centimeter and a lower peak of about 7×10^3 per cubic centimeter at 2200 kilometers. Data in the neutral atmosphere were obtained to a pressure level of about 120 millibars. The temperature structure derived from these data is consistent with the results of the Pioneer 11 Saturn infrared radiometer experiment (for a helium fraction of 15 percent) and with models derived from Earth-based observations for a helium fraction by number of about 4 to 10 percent. The helium fraction will be further defined by mutual iteration with the infrared radiometer team.*

The flight path of the Pioneer Saturn spacecraft during its encounter with Saturn on 5 September 1979 is described elsewhere in this issue (1). Near the closest approach point of its trajectory,

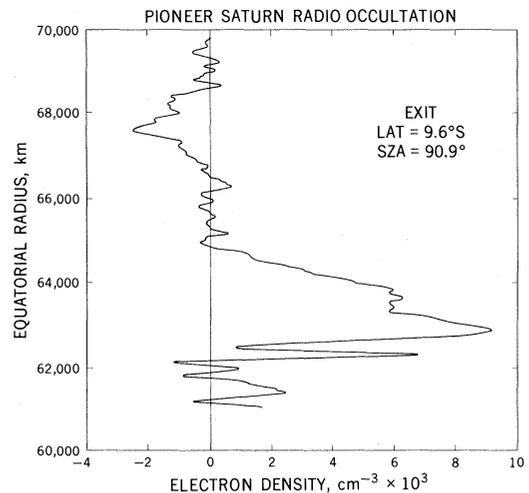
the spacecraft was occulted by Saturn at a distance of about 55,000 km from the occulting limb. The occultation tangency point was on the evening terminator at a latitude of about $11.5^\circ S$ and a solar ze-

nith angle (SZA) of about 89.2° . Before reaching the level at which significant refraction occurred, the spacecraft-to-Earth radio link was traveling through the atmosphere at a velocity of about 21.3 km/sec. About 1 hour 19 minutes later, the spacecraft emerged from behind the morning terminator limb when it was at a spacecraft-to-limb distance of about 120,500 km. The exit point was at a latitude of 9.6°S and an SZA of 90.6° . After emerging from the atmosphere, the spacecraft-to-Earth line of sight was traveling through the atmosphere at about 24.4 km/sec.

The results presented here were derived from bandwidth-reduced, digitally recorded data from the open-loop receivers at Deep Space Network stations 63 at Cebreros, Spain, and 14 at Goldstone, California. The digital recordings were produced by the occultation data assembly (ODA) (2) in which the open-loop receivers are referenced with a programmable local oscillator driven by computer-generated predictions based on the spacecraft orbit. The S-band (2.293 GHz) signal for the Pioneer spacecraft was digitally recorded in a bandwidth of about 8.3 kHz, sampled at a rate of 20,000 samples per second. Fast Fourier transform spectra were then computed from the digital data at intervals of 1 second to provide a local oscillator function. Using this local oscillator function and a transverse digital filter of 100-Hz bandwidth, we filtered the data and reduced the sample rate to 500 samples per second. These data were then passed through a signal detection program based on a digital second-order, phase-locked loop, in which the amplitude and frequency of the signal with respect to the local oscillator were computed and then combined with the local oscillator function to produce a time history of the frequency and amplitude of the signal present on the ODA recordings (3). Then the frequency ramps with which the programmed local oscillator of the ODA had been driven were introduced to reconstruct the actual "sky frequency" as it appeared at the receiver antenna.

We then removed the effects on the received frequency of the orbital motion of the spacecraft and the rotation of Earth by using frequency predictions based on the precisely determined orbit on the spacecraft (4). The resulting residuals then presumably represent the effects of propagation through Earth's atmosphere and ionosphere, the interplanetary medium, and the ionosphere and atmosphere of Saturn. Because the data were taken during a period of a few minutes, phase path changes, and hence frequency fluctuations,

Fig. 1. Electron density in the ionosphere of Saturn plotted against the equatorial radius. The negative region at a radius of about 68,000 km is probably indicative of the effect of solar wind disturbances and represents a measure of the uncertainty of the results.



due to changes in Earth's atmosphere and ionosphere can be expected to be negligible. This is not, however, the case with the interplanetary medium. At the time of the Pioneer Saturn encounter, the distance from the spacecraft to Earth was about 1.6×10^9 km, passing within about 8° of the sun at a time of high solar activity. This produced fluctuations in the frequency residuals due to the effects of a fluctuating number of solar wind electrons along the spacecraft-Earth line of sight.

The results described here were derived only from the data taken during the exit of Pioneer Saturn from occultation. At that time, the spacecraft transmitter was referenced by its onboard auxiliary oscillator, which had been in operation for about 1 hour 19 minutes after the uplink signal was lost during the entry oc-

cultation phase. The data from the entry occultation were taken in the three-way mode with a frequency reference provided by a signal transmitted to the spacecraft from DSN station 62. Because of the more complicated nature of the "three-way" data and because the transmitter frequency was ramped to counteract the high Doppler rates around Saturn periastris passage, the results of the entry measurements were not available for inclusion in this report.

Before the data can be inverted to produce geophysical quantities, any residual biases and drifts produced by modeling or by oscillator drift must be removed. We did this by least-squares fitting a straight line to a portion of the data presumably taken outside of the sphere of influence of the atmosphere and ionosphere of Saturn. Because of the solar

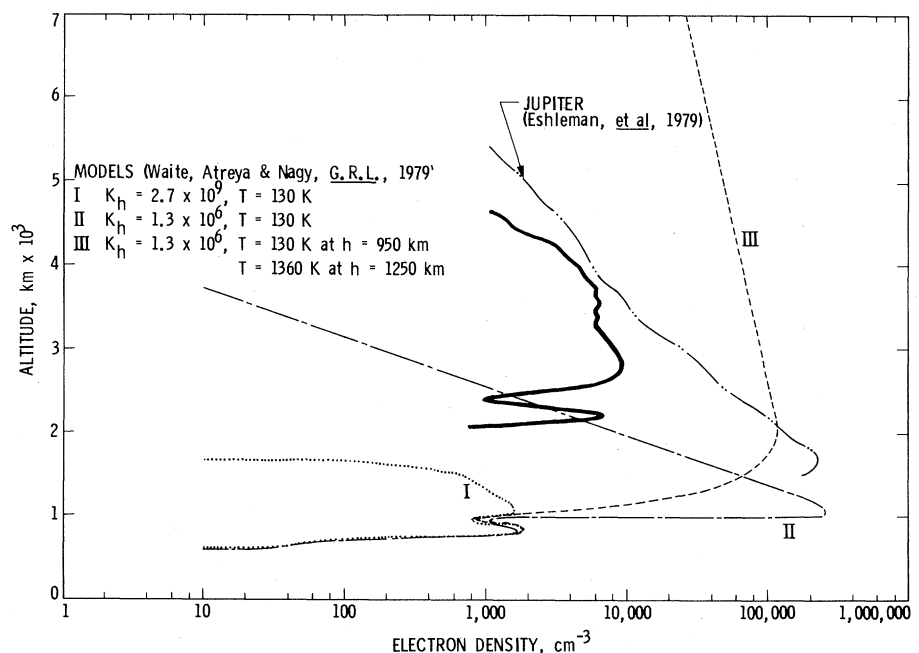


Fig. 2. Saturn radio occultation electron density profile (heavy line) plotted along with several predicted models (7). The peak electron density is less than one-tenth of that predicted.

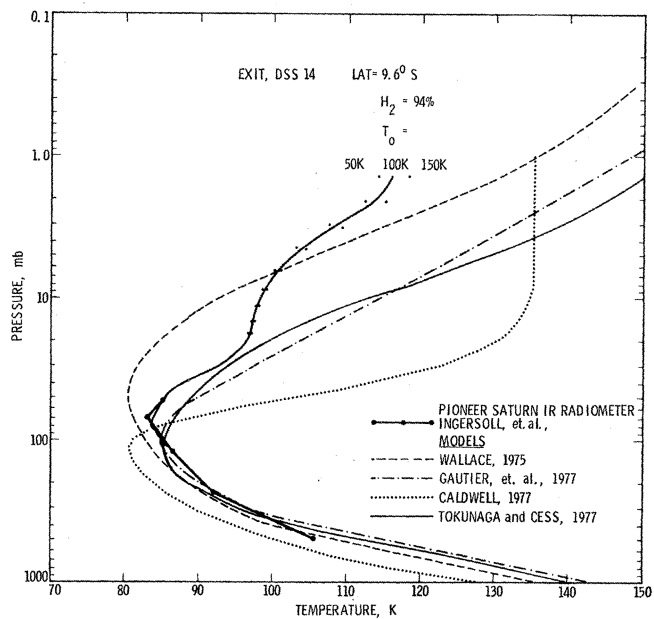
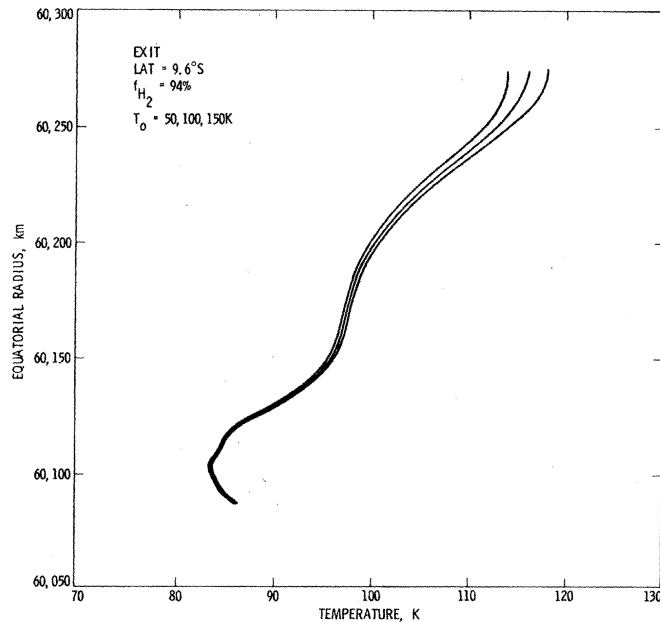


Fig. 3 (left). Temperature structure in the upper neutral atmosphere of Saturn, from a pressure level of about 1 to 120 mbar plotted against the equatorial radius. The measurement level just barely penetrates below the tropopause and into the convective region of the atmosphere. Fig. 4 (right). Pioneer 11 Saturn radio occultation results (heavy line with surrounding dots) shown with other data and models. The heavy line connecting the black dots represents the temperature structure derived from the Pioneer 11 Saturn infrared radiometer experiment (9). The four lighter curves represent models derived from ground-based observations (10). The radio occultation temperature profile shown here is for an assumed composition of 94 percent hydrogen and 6 percent helium by number. (The radio occultation curve stops at about 1.20 mbar.)

wind-induced fluctuations mentioned above, this was not an easy task. A drift function was produced which met the criterion that the frequency residual return to a near-zero value between the bottom of the ionosphere and the top of the neutral atmosphere. In essence, the drift function was produced by data taken at altitudes above 10,000 km, and all data downward of this point to the point of loss of signal were then referenced with this drift function and processed to obtain information on the ionosphere and atmosphere of Saturn.

The corrected data were used in conjunction with an ephemeris of the spacecraft relative to Saturn to obtain a history of the refractive bending angle as a function of the ray asymptote distance. The ray asymptote distance was computed with respect to a center of refraction which, because of the oblateness of Saturn, was located 2280 km from the center of figure. We computed the oblateness, and hence the location of the center of refraction, precisely by taking into account the rotation rate, mass, and gravity field coefficients of Saturn (4, 5). We then inverted these data by using the Abel integral transform to obtain a profile of refractivity as a function of radial distance (6).

In the ionosphere, the negative refractivity can be directly interpreted in terms of electron density. A profile of electron density in the ionosphere of Saturn derived from the exit measurement is shown in Fig. 1, plotted against equatorial radius. It is immediately obvious

that the electron densities in the Saturn ionosphere measured near the morning terminator are quite low, with a main peak only slightly in excess of 9000 cm^{-3} at an altitude of 2800 km and a lower peak of about 7000 cm^{-3} at about 2200 km.

The negative feature at about 68,000 km (Fig. 1) is probably an indication of the magnitude of the effects of the solar wind electrons along the ray path. This disturbance is about a quarter of the effect of the entire ionosphere, and this should provide an estimate of uncertainties in the measurement. The result of this measurement are compared with several models derived by Waite *et al.* (7) in Fig. 2; the heavy curve represents the Pioneer Saturn occultation measurement for the exit, plotted on a logarithmic scale. The altitude is measured from the level at which the neutral number density is 10^{19} cm^{-3} , which occurs at an equatorial radius of about 60,085 km and is the same as that used to compute the three models. In model I a low exosphere temperature of 130 K and a high value of the eddy diffusion coefficient K_h of 2.7×10^9 are assumed. This model yields a very low electron density ($\sim 1000 \text{ cm}^{-3}$) at an altitude of about 1000 km. Models II and III both assume a value of K_h consistent with observations of the ionosphere of Jupiter by the Pioneer and Voyager radio occultation experiments and represent extreme values of the scale height as determined by

exosphere temperatures of 130 K and 1360 K. The measured electron density profile does not conform to any of the three models, showing a maximum electron density lower by more than order of magnitude than those predicted from the models. Also shown in Fig. 2 is an electron density profile in the Jupiter atmosphere derived from the Voyager 1 radio occultation data (8). At the present stage of analysis, we believe that there is not sufficient information on the top-side scale height to attempt a computation of the exosphere temperature in that part of the Saturn upper atmosphere. It is not probable that the uncertainties of processing could produce a variation in the maximum electron density of more than a factor of 2. However, there is a remote possibility that the observed profile represents only the lower peak of a very gradual ionosphere extending beyond 10,000 km. This possibility will be explored in future processing.

In order to derive geophysical quantities such as temperature, pressure, and density in the neutral atmosphere, it is necessary to integrate the barometric equation downward from the point at which the refractivity becomes positive. To obtain density from refractivity, an assumption of the composition of the neutral atmosphere must be made. In addition, an initial temperature at the starting point of integration must be established. Then, for every data point, the perfect gas law is applied to obtain a temperature profile in the atmosphere.

During the Saturn encounter, the carrier signal strength margin was only about 18 dB above threshold. For this reason, the signal could only be followed to a level at which the closest approach distance of the ray corresponded to a pressure level of less than 120 mbar. It may be possible to extend the depth of penetration somewhat but certainly not to a great extent.

A profile of the temperature in the atmosphere of Saturn for a hydrogen fraction by number of 94 percent is shown in Fig. 3. The three separate curves represent initial temperatures at the top of the measurement of 50, 100, and 150 K. It is apparent that the depth of signal penetration was sufficient to carry measurements below the temperature minimum at the tropopause and slightly into the convective region of the atmosphere. The reason for choosing a hydrogen fraction of 94 percent becomes clearer upon examination of Fig. 4. The temperature-pressure structure of the Saturn atmosphere as determined from the Pioneer Saturn exit data is plotted alongside the temperature structure obtained from the Pioneer Saturn infrared radiometer experiment (9), as well as several models produced from Earth-based observations (10). The dots surrounding the Pioneer Saturn occultation profiles represent the effects of different assumptions with respect to the initial temperature. It should be noted that these are not error bars and should not be so interpreted. The actual error bars or uncertainty limits have not yet been established and they depend more on the subtleties of drift function fit than on the initial temperature assumptions.

The profile derived from the Pioneer Saturn radio occultation with the assumption of 94 percent hydrogen and 6 percent helium practically overlies the profile determined from the infrared radiometer measurements. The infrared radiometer profile has been derived assuming a helium fraction of 15 percent, and it will change somewhat as the helium fraction is varied. The location of the temperature minimum in the radio occultation profile is highly dependent on the composition. For instance, for 15 percent helium that minimum occurs at a temperature of about 91 K, and for 100 percent hydrogen it moves to about 79 K. This sensitivity to composition will eventually allow a good estimate of the ratio of hydrogen to helium to be made after several iterations with the Pioneer Saturn infrared radiometer results. Although it is premature at this stage of analysis to derive a helium fraction, it is obvious that the percentage of helium by

number cannot be higher than about 10 percent or lower than about 4 percent. Such a helium fraction is also consistent with the modeling of the interior structure of Saturn based on the mass and gravity coefficients derived from the celestial mechanics experiment (4). The structure in the temperature profile above the minimum is probably real, and the ledge at 10 to 30 mbar may represent heating by a layer of particles.

The analysis of data from the Pioneer Saturn radio occultation is continuing, and more information on the structure of the ionosphere and upper neutral atmosphere will be provided from the analysis of entry occultation data. These results will provide further clarification of the preliminary findings reported here, and in November 1980 radio occultation results at two frequencies will become available from the Voyager 1 flyby of Saturn. These results will most likely provide a deeper penetration into the neutral atmosphere.

ARVYDAS J. KLIORÉ
GUNNAR F. LINDAL
INDU R. PATEL
DONALD N. SWEETNAM
HENRY B. HOTZ

*Jet Propulsion Laboratory,
California Institute of Technology,
Pasadena 91103*

THOMAS R. McDONOUGH
*Pasadena Interdisciplinary Research,
Pasadena, California 91101*

References and Notes

1. J. Dyer, *Science* **207**, 400 (1980).
2. A. Berman and R. Ramos, *IEEE Trans. Geosci. Electron.*, in press.
3. R. Woo, W. Kendall, A. Ishimaru, R. Berwin, *Jet Propul. Lab Tech. Mem.* 33-644 (1973).
4. J. D. Anderson, G. W. Null, E. D. Biller, S. K. Wong, W. B. Hubbard, J. J. MacFarlane, *Science* **207**, 449 (1980).
5. A. J. Kliore and P. M. Woiceshyn, in *Jupiter*, T. Gehrels, Ed. (Univ. of Arizona Press, Tucson, 1976), p. 238.
6. G. Fjeldbo and V. R. Eshleman, *Planet. Space Sci.* **16**, 1035 (1968); A. J. Kliore, in *Mathematics of Profile Inversion*, L. Colin, Ed. (Publ. TMX-62, 150, National Aeronautics and Space Administration, Washington, D.C., 1972), p. 3-2.
7. J. H. Waite, Jr., S. K. Atreya, A. F. Nagy, *Geophys. Res. Lett.* **6**, 723 (1979).
8. V. R. Eshleman, G. L. Tyler, G. E. Wood, G. F. Lindal, J. D. Anderson, G. S. Levy, T. A. Croft, *Science* **204**, 976 (1979).
9. A. P. Ingersoll, G. S. Orton, G. Münch, G. Neugebauer, S. C. Chase, *ibid.* **207**, 439 (1980).
10. A. Tokunaga and R. Cess, *Icarus* **32**, 321 (1977); J. Caldwell, *ibid.* **30**, 493 (1977); L. Wallace, *ibid.* **25**, 538 (1975); D. Gautier, A. Lacombe, I. Rivah, *Astron. Astrophys.* **61**, 149 (1977).
11. We thank the Pioneer Project personnel at NASA/Ames Research Center, especially C. F. Hall, the project manager, and R. Hogan, J. Wolfe, and J. Dyer of his staff, for providing leadership in this important phase of the mission. We also express our gratitude to the personnel of the NASA-Jet Propulsion Laboratory (JPL) Deep Space Network, especially to R. B. Miller, A. Bouck, T. Howe, J. Wackley, and W. Hietzke for their help in acquiring the data, and to the JPL Pioneer navigation team led by W. Kirhofer and including W. Blume, S. K. Wong, E. Biller, and A. Lubeley for providing orbital data. Special thanks are due to P. Laing and D. Cain for adapting the prediction software and C. Conrad for help with data reduction. We also thank D. O. Muhleman, A. P. Ingersoll, and G. S. Orton for some useful discussions. The work described above represents the results of one phase of research at the Jet Propulsion Laboratory, California Institute of Technology, under NASA contract NAS 7-100. A.J.K. dedicates this report to the 400th anniversary of the University of Vilnius, Lithuania, the celebration of which took place while this work was in preparation.

3 December 1979

Pioneer Saturn Celestial Mechanics Experiment

Abstract. During the Pioneer Saturn encounter, a continuous round-trip radio link at S band (~ 2.2 gigahertz) was maintained between stations of the Deep Space Network and the spacecraft. From an analysis of the Doppler shift in the radio carrier frequency, it was possible to determine a number of gravitational effects on the trajectory. Gravitational moments (J_2 and J_4) for Saturn have been determined from preliminary analysis, and preliminary mass values have been determined for the Saturn satellites Rhea, Iapetus, and Titan. For all three satellites the densities are low, consistent with the compositions of ices. The rings have not been detected in the Doppler data, and hence the best preliminary estimate of their total mass is zero with a standard error of 3×10^{-6} Saturn mass. New theoretical calculations for the Saturn interior are described which use the latest observational data, including Pioneer Saturn, and state-of-the-art physics for the internal composition. Probably liquid H_2O and possibly NH_3 and CH_4 are primarily confined in Saturn to the vicinity of a core of approximately 15 to 20 Earth masses. There is a slight indication that helium may likewise be fractionated to the central regions.

A continuous round-trip coherent radio link at S band (~ 2.2 GHz) was maintained between the Pioneer spacecraft and stations of the Deep Space Network (DSN) during the period from 17 August to 4 September 1979. When the spacecraft passed behind Saturn, which started about 62 seconds after closest ap-

proach on 1 September, radio contact with Pioneer was lost and consequently there is a 97-minute gap in the round-trip data shortly after closest approach. Nevertheless, by analyzing the Doppler shift in the radio carrier frequency outside of occultation, one can measure trajectory perturbations on the spacecraft and de-